A Light Scattering Study on the Droplet Size and Interdroplet Interaction in Microemulsions of AOT–Oil–Water System

M. J. HOU, M. KIM, AND D. O. SHAH*

Center for Surface Science and Engineering, Departments of Chemical Engineering and Anesthesiology, University of Florida, Gainesville, Florida 32611

Received March 30, 1987; accepted June 21, 1987

Quasi-elastic light scattering and static light scattering techniques were used to study the droplet size and interdroplet interaction in W/O microemulsions consisting of AOT, oil, and water. The intrinsic diffusion coefficients and the virial coefficients were determined by extrapolating the experimental data to infinite dilution and studied as functions of the following variables: the molar ratio of water to surfactants, the chain length of oil, salinity, and the ratio of nonionic surfactant, Arlacel-20, to AOT. Time-averaged intensity data were interpreted based on the theory of hard sphere model with a small perturbation due to attractive interaction between the spheres. It was found that the droplet size and the interdroplet attractive interaction increased with the molar ratio of water to AOT and the chain length of oil. In contrast, an increase in salinity decreased the droplet size and interdroplet attractive interaction. The addition of Arlacel-20 increased the droplet size but decreased the strength of the attractive interaction between microemulsion droplets. In addition to the dilution procedure, the angle-dependent measurements were also made and the data were analyzed by a square well attractive potential. It is emphasized that one must be cautious of the inaccuracy of angle-dependent analysis, since the dependence of diffusion coefficients on angle in microemulsions is usually very weak and within the experimental error.

I. INTRODUCTION

Microemulsions are thermodynamically stable, isotropic dispersions consisting of microdomains of oil and/or water stabilized by an interfacial film of surface active molecules (1). Due to their importance in the application in enhanced oil recovery, pharmaceutics, and cosmetics, microemulsions have been extensively studied using X-ray and light scattering, ultracentrifugation, spin label probes, dielectric relaxation, fluorescence probes, and neutron scattering (2–15). The microstructure of such microemulsions has been described as spherical droplets of water in oil or oil in water, depending on the nature of the surfactants used and the composition of microemulsions. However, it has been reported that for certain compositions these isotropic microemulsions may also exist as other structures such as bicontinuous (16, 17) or cubic (18) structure. The characterization of the size and shape of the microemulsion droplets and the mutual interaction between these droplets has been vigorously pursued recently. Several researchers have shown that the droplet size and the interdroplet interaction can vary over a wide range by changing the composition of the microemulsion (15, 19–26). In most of these studies, modern theories of liquids have been applied to analyze the light scattering data to determine the values of some parameters such as osmotic compressibility, virial coefficients, and diffusion coefficient. Such an approach has been applied to several quaternary systems containing single chain surfactants where the presence of short chain alcohol is essential to maintain the phase stability of microemulsions (19–25).

It has been known for about a decade that the anionic surfactant sodium di-2-ethyl-hexyl sulfosuccinate, or Aerosol OT (AOT), can

* To whom all correspondence should be addressed.

0021-9797/88 $3.00

form a thermodynamically stable microemulsion without addition of short chain alcohols. This realization has distinguished this system as a suitable reference for fundamental studies on microemulsions. Although numerous efforts (27–29) have been made to study the structure, dynamics, and reaction in such microemulsions (mostly with the continuous oil being isooctane or *n*-heptane), few systematic studies (26, 30–32) were undertaken regarding the droplet size and the interdroplet interactions. The chemical structure of oil, salinity, and the amount of water (19–25) have been found to affect profoundly the droplet size and the interdroplet interaction in quaternary systems containing single chain surfactants. However, the interpretation of above effects was sometimes complicated by the associated variation in alcohol partitioning between interface and continuous phase. Therefore, it is essential to systematically investigate the above effects in the absence of alcohols. In this regard, microemulsions containing AOT are excellent ternary systems for such a study. On the other hand, short chain alcohols and nonionic surfactants have been used as cosurfactants in the formulation of quaternary microemulsion systems. Hence, it is also interesting to know the influence of such additives on the droplet size and the interdroplet interaction in AOT-containing microemulsions.

Furthermore, in most of the light scattering studies reported so far, the analysis of light scattering data in terms of size and interaction usually required the extrapolation of the experimental data to infinite dilution. For microemulsion systems where a substantial amount of alcohol is present, this approach usually involves a tedious titration procedure to ensure the constancy of both the size and the composition of microemulsion droplets during dilution (33, 34). For the microemulsion systems where only a very small amount of alcohol is present, this titration procedure becomes very difficult and inaccurate. Recently, angle-dependent quasi-elastic light scattering (QELS) data have been analyzed (35), without resort to extrapolation, to determine the hydrodynamic radius of microemulsions. The current study also examined the feasibility of applying such an approach to extract the information about the droplet size and the interdroplet interaction of microemulsions.

II. EXPERIMENTAL

II.1. Sample Preparation

Table I shows the specific composition of all the samples studied. The volume fraction, ϕ, of the dispersed phase was defined as $\phi = (V_s + V_w)/V$ where V is the total volume of the mixture, V_s the volume of surfactant added (obtained by dividing the weight with the density of surfactant, 1.13 g/ml), and V_w the volume of water added. The oils used were from Fisher Scientific (99 mole% pure), as was NaCl (Certified ACS grade). The alcohols were purchased from Sigma (99 mole% pure). Arlacel-20 (Sorbitan monolaurate) was from ICI. AOT was purchased from Sigma (99% sodium salt). All ingredients were used without further purification.

Before light scattering measurements, the sample was injected into a clean cylindrical cell directly through a syringe filter with a 0.2-μm PFT membrane. The cell was thoroughly cleaned by the following procedure: soak in concentrated sulfuric acid and soap solution successively, wash with tap water, rinse with filtered distilled water, then dry in oven. The sample was maintained at 20 ± 0.1°C during measurement.

II.2. Light Scattering Measurements

The optical source of the light scattering apparatus was a Spectra Physics argon ion laser (Model 2000) operating at 514.5 nm. The scattered light was collected at the appropriate angle by a laser light scattering goniometer (Model 200SM) and was focused on a photomultiplier cathode (EMI-9865), both from Brookhaven Instrument. For most of the study the scattering angle was fixed at 90° except for an angle-dependent measurement where the

TABLE I

Composition of the Samples Studied

Samples[a]	Oil	n_w/n_s	Salinity (wt%)	Additive	Additive/AOT (mole/mole)
C_5-W-20	*n*-Pentane	20	—	—	—
C_7-W-20	*n*-Heptane	20	—	—	—
C_7-W-40	*n*-Heptane	40	—	—	—
C_7-W-60	*n*-Heptane	60	—	—	—
C_{10}-W-20	*n*-Decane	20	—	—	—
C_{10}-W-30	*n*-Decane	30	—	—	—
C_{10}-W-40	*n*-Decane	40	—	—	—
C_{10}-W-20-P(0.38)	*n*-Decane	20	—	*n*-Propanol	0.38
C_{10}-W-20-H(0.47)	*n*-Decane	20	—	*n*-Heptanol	0.47
C_{12}-W-20	*n*-Dodecane	18.5	—	—	—
C_{12}-B(0.5%)-20	*n*-Dodecane	20	0.5	—	—
C_{12}-B(1%)-20	*n*-Dodecane	20	1.0	—	—
C_{12}-W-20-A(0.44)	*n*-Dodecane	20	—	Arlacel-20	0.44
C_{12}-W-20-A(0.99)	*n*-Dodecane	20	—	Arlacel-20	0.99

[a] Abbreviations used in sample codes: W, water; B, brine (% indicates NaCl % (w/w) in the aqueous solution); A, Arlacel-20; P, propanol; H, heptanol.

angle was varied from 30° to 150°. The time-averaged intensity and time-dependent correlation function of the scattered intensity were recorded by using a fast clipped real time correlator (Model BI 2030) with 72 channels and a time resolution of 100 ns. The excess scattering intensity was determined by using benzene as the reference. Correlation time was measured within 5%. During the measurement of the time correlation of intensity, the data were rejected to avoid any error caused by dust contamination if the difference between the calculated and measured baselines was greater than 0.2%. The normalized correlation function of scattered electric field, $g^{(1)}(t)$, was analyzed using the method of cumulant (35–37), in which the logarithm of the normalized $g^{(1)}(t)$ was fitted to a polynomial equation using a nonlinear least-squares fitting routine. The fitting equation is described as

$$\ln[(c_1 b)^{1/2} g^{(1)}(t)] = \ln(c_1 b)^{1/2} - \Gamma t + \mu_2(t^2/2!),$$

where c_1 and b are baseline and instrument constant. The first cumulant of linewidth distribution, Γ, is equal to Dq^2. The second cumulant of linewidth distribution is μ_2. The magnitude of scattering vector, q, is defined as $q = (4\pi n_0/\lambda_0)\sin(\theta/2)$, where n_0 is the refractive index of continuous medium, λ_0 the wavelength of light under vacuum, and θ the scattering angle.

III. RESULTS AND DISCUSSION

III.1. THEORETICAL BACKGROUND

III.1.1. Analysis of QELS Data in Terms of Interaction and Size

Modern theories of liquids have been used successfully by several researchers (15, 19–26) to explain the light scattering data of W/O microemulsions. These authors have shown that the light scattering intensity of W/O microemulsions can be well interpreted by a hard sphere potential, U_{hs}, with a perturbation of attractive potential, U_a. Thus, the osmotic pressure, Π, can be expressed as

$$\Pi = \Pi_{hs} + \Pi_a. \quad [1]$$

The osmotic pressure of hard sphere, Π_{hs}, can be accurately described by the Percus–Yevick (38)–Carnahan–Starling (39) approximation via

$$\Pi_{hs} = \frac{kT\phi_{hs}}{v_{hs}} \frac{1 + \phi_{hs} + \phi_{hs}^2 - \phi_{hs}^3}{(1 - \phi_{hs})^3}, \quad [2]$$

where v_{hs} and ϕ_{hs} are the individual volume and volume fraction of hard sphere, k is the Boltzmann constant, and T is absolute temperature. The attractive perturbation of osmotic pressure can be written as (40)

$$\Pi_a = (\phi_{hs}/v_{hs})^2 2\pi \int_0^\infty U_a(r) g_{hs}(r) r^2 dr + \text{higher order terms,} \quad [3]$$

where r is the separation distance between the centers of two spheres and $g_{hs}(r)$ the radial distribution function of hard spheres. If we neglect the higher-order terms, Eq. [3] becomes

$$\Pi_a = (\phi_{hs}/v_{hs})^2 2\pi \int_\sigma^\infty U_a(r) r^2 dr = (kT/v_{hs})(A\phi_{hs}^2/2), \quad [4]$$

where σ is the diameter of a hard sphere and

$$A = 4\pi/(kTv_{hs}) \int_\sigma^\infty U_a(r) r^2 dr. \quad [5]$$

Therefore, from Eqs. [1], [2], and [4], we have (41)

$$\Pi = \frac{kT}{v_{hs}} \left\{ \frac{\phi_{hs}(1 + \phi_{hs} + \phi_{hs}^2 - \phi_{hs}^3)}{(1 - \phi_{hs})^3} + \frac{A\phi_{hs}^2}{2} \right\}. \quad [6]$$

The osmotic pressure can be related to the excess scattering intensity at 90°, R_{90}, via

$$R_{90} = KkT\phi(\partial\Pi/\partial\phi)^{-1}, \quad [7]$$

where $K = 2\pi^2 n^2 \lambda^{-4} (\partial n/\partial\phi)^2$, ϕ is the volume fraction of microemulsion droplets, and n is the refractive index of microemulsions. Let $a = \phi_{hs}/\phi$ and substitute Eq. [6] into [7]; we obtain

$$R_{90} = \frac{Kv_m\phi(1 - a\phi)^4}{(1 + 2a\phi)^2 - (a\phi)^3(4 - a\phi) + Aa\phi(1 - a\phi)^4}, \quad [8]$$

where v_m is the volume of a microemulsion droplet. One can also express the osmotic pressure, Π, of microemulsions as a function of different powers of the volume fraction of microemulsion droplets, according to the virial formula,

$$\Pi = (\phi kT/v_m)(1 + B\phi/2 + C\phi^2/3 + \cdots), \quad [9]$$

where B and C are the second and third virial coefficients of osmotic pressure. From Eqs. [6] and [9], one can show that, for small ϕ, B can be approximately related to a and A by (19)

$$B = a(8 + A). \quad [10]$$

The Brownian motion of these interacting droplets can be studied by QELS to determine the diffusion coefficient, D. In the low concentration range, D can be written as

$$D = D_0(1 + \alpha\phi), \quad [11]$$

where D_0 is the intrinsic diffusion coefficient at infinite dilution. From the Stokes–Einstein relationship, one can determine the hydrodynamic radius, R_H, of the microemulsion droplets as

$$R_H = kT/(6\pi\eta D_0), \quad [12]$$

where η is the viscosity of the continuous medium. The virial coefficient of diffusion, α, is related to the interacting potential, $U(r)$, via the equations (42)

$$\alpha = B - \beta \quad [13]$$

$$B = (4\pi/v_m) \int_0^\infty \{1 - \exp[-U(r)/(kT)]\} r^2 dr = 8 + 24 \int_1^\infty \{1 - \exp[-U(x)/(kT)]\} x^2 dx \quad [14]$$

$$\beta = \beta_0 + \int_1^\infty F(x)\{1 - \exp[-U(x)/(kT)]\} dx, \quad [15]$$

where $x = r/(2R_{hs})$, R_{hs} is the hard sphere radius. Felderhof (43) has found that

$$\beta_0 = 6.44$$

and

$$F(x) = 12x - 15/(8x^2) + 27/(64x^4) + 75/(64x^5). \quad [16]$$

From Eqs. [8], [10], [11], and [12], it appears that R_H, α, a, A, and B can be extrapolated

from the study of D and R_{90} as functions of ϕ in the low concentration range. Such efforts have been attempted in quaternary systems by several researchers (15, 19–23). In all of these studies, as mentioned before, a tedious titration procedure must be employed. The validity and limitation of such a titration procedure have been verified and discussed by Dvolaitzky *et al.* (15) and Cazabat (44). Nevertheless, in the case where only a very small amount of alcohol is present, this procedure may become difficult and inaccurate.

Recently, Chang and Kaler (35) have presented an alternative approach to determine the droplet size by analyzing the q-dependent apparent diffusion coefficient, $D(q)$. This method mainly involves fitting the q-dependent data with Fijnaut's equations (45). Following Felderhof's work (43), Fijnaut (45) has derived, in the limit of stick boundary conditions (i.e., no-slip conditions) at the surface of particles, a relation between the measured q-dependent D and D_0, i.e.,

$$D(q) = D_0\{1 + \phi[S_1(q) + H_1 + H_2(q)]\}, \quad [17]$$

where

$$S_1(q) = 3/(qR_H)^3 \int_0^\infty x \sin x[1 - g(x/q)]dx \quad [18]$$

$$H_1 = (27/8)R_H^3 \int_0^\infty g(x)x^{-4}dx - (15/4)R_H \int_0^\infty g(x)x^{-2}dx \quad [19]$$

$$H_2(q) = (9/2)/(qR_H)^2 \int_0^\infty (\sin x + \cos x/x - \sin x/x^2)[g(x/q) - 1]dx + 3\int_0^\infty (3 \sin x/x^4 - 3 \cos x/x^3 - \sin x/x^2)g(x/q)dx + (225/4)(qR_H)^4 \times \int_0^\infty (\sin x/x^6 + 2 \cos x/x^7 - 2 \sin x/x^8)g(x/q)dx, \quad [20]$$

where $g(x)$, the radial distribution function, is directly related to the interaction potential by

$$g(x) = \exp[-U(x)/(kT)]. \quad [21]$$

From Eqs. [17] to [21], it is clear that with a suitable potential function describing the mutual interaction between microemulsion droplets, hydrodynamic radius R_H can be determined without resorting to the tedious dilution.

III.1.2. Interaction Potentials

Recently, Chang and Kaler (35) have applied a hard sphere model to Fijnaut's results to analyze q-dependent QELS results. Because of the hard sphere model they assumed, no information about the interdroplet interaction could be obtained, so only droplet size was determined. Several researchers have shown that the interaction in microemulsions can vary from a very strong attraction to a very weak one (15, 19–23) by changing the droplet size and the fluidity of the interface of microemulsion droplets. The origin of these interactions has been discussed in the past (22, 25). Calje *et al.* (25) have proposed that these interactions are the result of the difference in the molecular composition between the droplets and the continuous medium. However, the application of Hamaker's work to the W/O microemulsion by Vrij *et al.* (25) led to a very weak interaction potential, when realistic values were assumed for the Hamaker constant. In order to explain this inconsistency, Vrij *et al.* (25) suggested that the interpenetration of microemulsion droplets should be taken into account. Such modification has been carried out by Lemaire *et al.* (46) in their recent derivation of a mean field intermicellar potential which includes both energetic and entropic contributions. A detailed calculation by these authors has shown that the most important contribution to the attractive interaction occurred in the overlapping region during the interpenetration of two droplets. Despite the success in explaining the significant features of interaction, the form of this potential function is very cumbersome and difficult

to apply to Fijnaut's results, i.e., Eqs. [17] to [20]. For the purpose of calculation, we applied a simple square well attractive potential function to describe the interdroplet interaction in this study. That is,

$$U(r) = \begin{cases} 0, & \sigma_H < r \\ -\epsilon, & \sigma < r < \sigma_H \\ \infty, & r < \sigma, \end{cases} \quad [22]$$

where ϵ is the uniform depth of attractive interaction, σ is the hard sphere diameter, and σ_H is the hydrodynamic diameter of the droplets. It is noted that the attractive interaction described by Eq. [22] is short-range in nature. Thus Eq. [22] retained the significant feature pointed out by Lemaire *et al.* (46, 47); that is, the most important contribution to the attractive interaction comes from the overlapping region. It is also worthwhile to point out that Vrij *et al.* (25) have applied a square well potential to interpret their scattering intensity data with considerable success. In their case, the width of the attraction well was found to be equivalent to the typical thickness of the surfactant layer.

III.1.3. Derivation of Equations for q-Dependent Analysis

Substituting Eq. [22] into Eqs. [13] to [16], we obtained

$$B = 8 + 8\{1 - \exp[\epsilon/(kT)]\}(\xi^3 - 1)dx \quad [23]$$

$$\beta = \beta_0 + \int_1^{\xi} F(x)\{1 - \exp[\epsilon/(kT)]\}dx, \quad [24]$$

where $\xi = \sigma_H/\sigma$. Again, substituting Eq. [22] into Eqs. [17] to [20], we obtained

$$D(q) = D_0\{1 + \phi[(S_1(q) + H_1 + H_2(q)]\} \quad [25]$$

$$S_1(q) = 3/(qR_H)^3[1 - \exp(\epsilon/(kT))] \times [\sin(q\sigma_H) - (q\sigma_H)\cos(q\sigma_H)] + \exp[\epsilon/(kT)][\sin(q\sigma) - (q\sigma)\cos(q\sigma)] \quad [26]$$

$$H_1 = [1 - \exp(\epsilon/(kT))][(9/8)(R_H/\sigma_H)^3 - (15/4)(R_H/\sigma_H)] + \exp[\epsilon/(kT)] \times [(9/8)(R_H/\sigma)^3 - (15/4)(R_H/\sigma)] \quad [27]$$

$$H_2(q) = (9/2)(qR_H)^2 I_1 + 3I_2 + (225/4)(qR_H)^4 I_3, \quad [28]$$

where

$$I_1 = [1 - \exp(\epsilon/(kT))][\cos(q\sigma_H) - \sin(q\sigma_H)/(q\sigma_H)] + \exp[\epsilon/(kT)][\cos(q\sigma) - \sin(q\sigma)/(q\sigma)]$$

$$I_2 = [1 - \exp(\epsilon/(kT))][\sin(q\sigma_H)/(q\sigma_H)^3 - \cos(q\sigma_H)/(q\sigma_H)^2] - \exp[\epsilon/(kT)][\sin(q\sigma)/(q\sigma)^3 - \cos(q\sigma)/(q\sigma)^2]$$

$$I_3 = [1 - \exp(\epsilon/(kT))]\{(2/7)[\cos(q\sigma_H)/(q\sigma_H)^6 - \sin(q\sigma_H)/(q\sigma_H)^7] + (5/7)\int_{q\sigma_H}^{\infty} (\sin x)x^{-6}dx\} + \exp[\epsilon/(kT)]\{(2/7)[\cos(q\sigma)/(q\sigma)^6 - \sin(q\sigma)/(q\sigma)^7] + (5/7)\int_{q\sigma}^{\infty} (\sin x)x^{-6}dx\}.$$

Equations [23] to [28] were used to interpret the angle-dependent data in this study.

III.2. Results Obtained by Dilution Procedure

III.2.1. Diffusion Coefficient Measurements

We have measured the apparent diffusion coefficient, D, at varying volume fractions, ϕ. The intrinsic diffusion coefficient, D_0, and the virial coefficient of diffusion, α, were obtained by extrapolating the data to infinite dilution, i.e.,

$$D_0 = \lim_{\phi \to 0} D$$

$$\alpha = \lim_{\phi \to 0} (\Delta D/\Delta\phi).$$

In extrapolation, the linear regression was applied to the linear portion of the data to determine the slope and intercept. Note that, for practical purposes, we have assumed that all surfactant molecules were adsorbed on the in-

terface of microemulsion droplets. Therefore, the samples can be directly diluted to the desired volume fraction with the continuous component, oil. The validity of such an assumption is discussed in a later section. In this part of the study, the above procedure was repeated for different series of experiments by changing n_w/n_s, molar ratio of water to surfactant, salinity, and the chain length of oil, and by adding the long chain nonionic surfactant, Arlacel-20. The results are summarized in Table II. For comparison, the diffusion coefficients were plotted as a function of ϕ for different series of experiments as shown in Figs. 1 to 4. Note that the diffusion coefficients have been normalized by dividing with D_0 for convenience of presentation. We now discuss the results as follows.

III.2.1.a. Effect of water solubility. Three samples of microemulsion consisting of AOT–*n*-heptane–water, with n_w/n_s being 20, 40, and 60, were studied. The volume fraction dependence of D has also been studied by Gulari *et al.* (30–31) and Nicholson and Clarke (32) using the same system. These authors reported that for $n_w/n_s = 20$, R_H is 45 Å at 25°C (32), while for $n_w/n_s = 60$, R_H's are 112 and 127 Å at 15 and 25°C, respectively (30). Thus, the hydrodynamic radii determined in this study as shown in Table II are in good agreement with those from Refs. (30–32). The hydrodynamic radius, R_H, increased with the value of n_w/n_s, as expected. It is easy to show (48) that $V_w = RA/3$, where V_w is the volume of solubilized water, R the radius of water core, and A total interfacial area. Therefore, the linear increase in R_H suggests that the interfacial area occupied per surfactant molecule is approximately the same and independent of the amount of water added, if the surfactant concentration is fixed as pointed out by Nicholson and Clarke (32). Figure 1 also shows that the slope of D/D_0 vs ϕ plot became more negative, indicating that the interdroplet interaction became more attractive, as the value of n_w/n_s increased (droplet size increased). This result is consistent with the general concept (49) that the magnitude of interaction increases with the radius of droplets. Such a finding is also in parallel with the results reported on the quaternary systems containing single chain surfactants (19, 20, 23, 47). The absolute value of intrinsic diffusion coefficients, D_0, and the virial coefficient, α, obtained from extrapola-

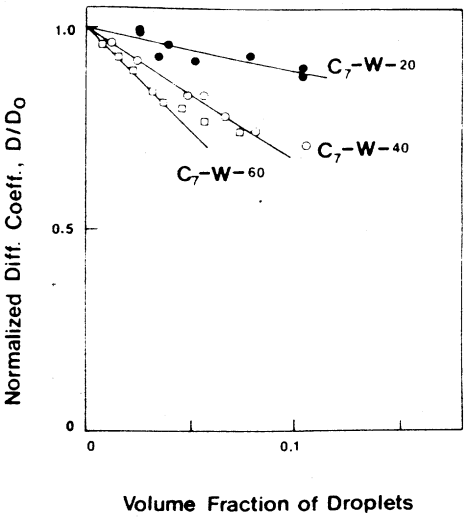

FIG. 1. The effect of n_w/n_s on the diffusion coefficients of microemulsion AOT–*n*-heptane–water.

TABLE II

Summary of the Results Obtained by Extrapolation

Samples	$D_0 \times 10^7$ (cm²/s)	R_H (Å)	α
A. Effects of n_w/n_s			
C_7-W-20	13.0110	40.3	−1.1
C_7-W-40	6.2414	84.0	−3.6
C_7-W-60	4.3871	119.5	−5.1
B. Effects of oil chain length			
C_5-W-20	25.2310	35.4	−0.6
C_7-W-20	13.0110	40.3	−1.1
C_{10}-W-20	3.8524	60.0	−4.7
C_{12}-W-20	2.3587	62.3	−13.9
C. Effects of salinity			
C_{12}-W-20	2.3587	62.3	−13.9
C_{12}-B(0.5%)-20	2.4996	58.8	−5.7
C_{12}-B(1%)-20	2.7788	52.9	−4.1
D. Effect of Arlacel-20			
C_{12}-W-20	2.3587	62.3	−13.9
C_{12}-W-20-A(0.44)	2.2042	66.7	−5.4
C_{12}-W-20-A(0.99)	1.9331	76.0	−0.3

tion were also reported in Table II, along with those from the studies of other samples. Nicholson and Clarke (32) have reported that $\alpha = -2.1$ independent of the value of n_w/n_s, which would be in conflict with the results of this study and also inconsistent with those from the studies in quaternary systems containing single chain surfactant (19, 20, 23, 47). The discrepancy may be due to the fact that they determined the slope based on a very wide concentration range (up to $\phi = 0.4$). The validity of applying Eq. [11] to such high concentrations is certainly debatable.

III.2.1.b. Effect of oil chain length. In this part of the study, four samples with oil, *n*-pentane, *n*-heptane, *n*-decane, and *n*-dodecane, were studied. When n_w/n_s was fixed at 20, the hydrodynamic radius was found to increase as the chain length of oil increased (see Table II). From the consideration of the geometric packing at the interface, longer chain length of oil has more difficulty in penetrating into the surfactant layer. As a result, the interface would favor a smaller curvature, as pointed out by Israelachvili *et al.* (50). Thus, there is a small increase in the radius of droplets, as the chain length of oil is increased, even though the molar ratio of water to AOT was constant. On the other hand, the interdroplet interaction was increased strikingly by the increase of oil chain length. As shown in Fig. 2, the virial coefficient of diffusion, α, decreased dramatically as the chain length of oil increased. This observation is also consistent with the results from the studies on the microemulsion containing single chain surfactant by other researchers (20, 47). According to Lemaire *et al.* (46) and Roux *et al.* (47), the magnitude of attraction between droplets increased with the difference between the composition of interface and continuous phase. The increasing difficulty in penetrating the interface by larger oil molecules would increase this difference, thus increasing the magnitude of interaction, which is consistent with the experimental results.

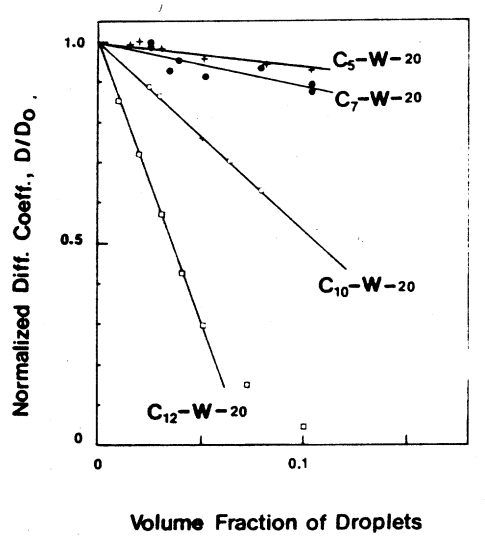

FIG. 2. The effect of oil chain length on the diffusion coefficients.

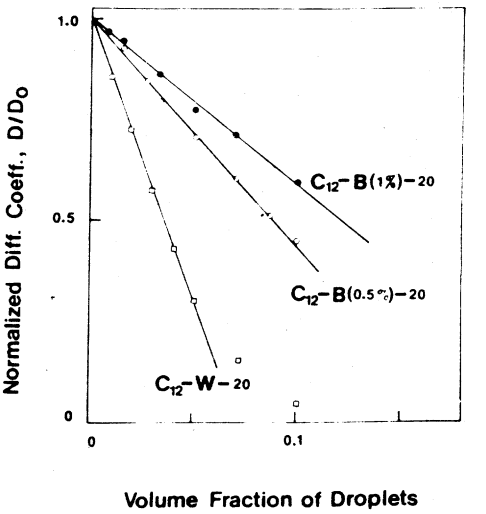

FIG. 3. The effect of salinity on the diffusion coefficients of microemulsion AOT–*n*-dodecane–water (or brine).

III.2.1.c. Effect of salinity. The effect of salinity was investigated by replacing water with an NaCl solution of different salinity (0.5 and 1 wt% in water) in microemulsions of AOT–*n*-dodecane–water. As shown in Fig. 3 and Table II, the interdroplet interaction became less attractive and the hydrodynamic radius decreased as the salinity of water was increased. The effect of salinity in quaternary systems containing single chain surfactant has been studied by Cazabat and Langevin (19). These authors reported that the interdroplet

interaction became less attractive and the droplet size increased slightly or remained unchanged in some cases, as the salinity increased. However, they also pointed out that these effects were associated with the change in the partitioning of alcohols at the interface, which makes it difficult to draw a clear conclusion for the role of salinity.

Since no such ambiguity was present in our system which consisted of AOT, water, and oil, it is obvious that the observed results can be ascribed to the screening of the electrostatic forces in the presence of salt. That is, an increase of salinity decreases the interfacial area per polar head of surfactant molecules and makes the interface more rigid and less penetrable. Thus the strength of attractive interaction decreases. The decrease of area per polar head group also favors a greater curvature of interface. Thus, when the salinity increases, the droplet size decreases in W/O microemulsions.

The effect of salinity has also been extensively studied by Bedwell and Gulari (26) in AOT–*n*-heptane–water system. From both static and dynamic light scattering data, the Hamaker constant and droplet size have been determined by these authors. They reported that the attractive interaction was decreased upon addition of small amounts of NaCl, which is consistent with our observation. They also pointed out that the reduction of attraction can also be explained, in addition to the condensation of surfactant film, by the decreasing magnitude of the fluctuation of the dipoles (developed around droplets) on increasing salinity. However, they did not observe any change in the droplet size upon increasing salinity from 0 to 3%. Such an observation is somewhat surprising since one would expect a greater interfacial curvature when salinity is increased as predicted theoretically by many thermodynamic considerations (50–52). A possible explanation may reside in the differences in these two systems. By using a small oil molecule (*n*-heptane) and less water (n_w/n_s = 4 to 12), the interfacial area occupied by each surfactant molecule is already smaller; hence the effect of condensation of interfacial film on the droplet radius is probably less significant.

III.2.1.d. Effect of nonionic surfactant Arlacel-20. We have also studied the effect of addition of nonionic surfactant Arlacel-20 to microemulsions consisting of AOT–dodecane–water. When short chain alcohols were added to the microemulsion containing single chain surfactants, the magnitude of attractive interaction was generally found by several authors to increase (19, 20, 23, 47). It is believed that the addition of alcohols increases the interfacial flexibility (or fluidity), so that the degree of interpenetration of droplets increases during the collision of the droplets. Thus, one would expect that the addition of long chain nonionic surfactant, Arlacel-20, should make the interface more rigid and decrease the strength of attraction between microemulsion droplets. Indeed, this was confirmed by the experimental results, as shown in Fig. 4, where the slope of D/D_0 vs ϕ plot became less negative as the molar ratio of Arlacel-20 to AOT was increased. From Table II, it appears that the addition of Arlacel-20 increased the droplet size significantly. The increase in droplet size can be ascribed to the big polar head of Arlacel-20. The insertion of this big polar head into

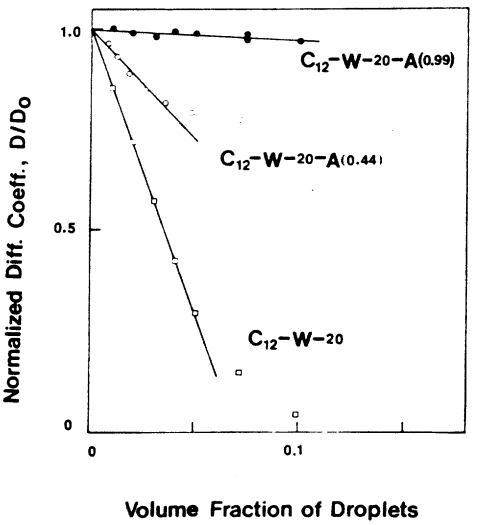

FIG. 4. The effect of Arlacel-20 on the diffusion coefficients of microemulsion AOT–*n*-dodecane–water.

the interface would be expected to increase the area per surfactant molecule and favor a smaller curvature of interface and hence a larger droplet radius.

III.2.2. Intensity Measurements

The validity of Eq. [8] to interpret the intensity data has been demonstrated by several researchers (19–26), since its theoretical basis was first developed by Calje *et al.* (25). By fitting intensity data with Eq. [8], one can determine several important parameters, A and a, from which the second virial coefficient B and hard sphere radius can be deduced. Such a procedure has been applied to several different samples so that the effects observed in the preceding section can be further examined. Since the effect of salinity on droplet interaction has been extensively studied by Bedwell and Gulari (26) in an AOT–*n*-heptane–brine system using essentially the same approach, the salinity effect was not repeated in intensity measurements. We studied the system, AOT–*n*-decane (or *n*-dodecane)–water and the fitting of data is generally good as shown in Figs. 5 and 6. From Table III, we found that the value of the second virial coefficient decreased as n_w/n_s increased or alkane chain length increased, while the addition of Arlacel-20 increased the value of B. Thus, this result further supports our previous conclusions on the effects of n_w/n_s, oil chain length, and nonionic surfactant on interdroplet interactions. The observed difference between R and R_{hs} ranged from 3.3 to 6.4 Å except one sample, C_{12}-W-20-A(0.44), where only 1.1 Å was observed. This result is very close to the one obtained in AOT–*n*-heptane–water (4 to 7.5 Å). Kotlarchyk *et al.* (53) have shown that the thickness of the AOT tail layer in swollen reversed micelles is about 10.4 Å with a distance of 2.4 Å penetrated by oil. Bedwell and Gulari (26) have explained this difference by assuming that the hard sphere radius extended all the way to the ester group of surfactants. Viewed from another angle, the differences obtained are also consistent with the range of interaction potentials reported by

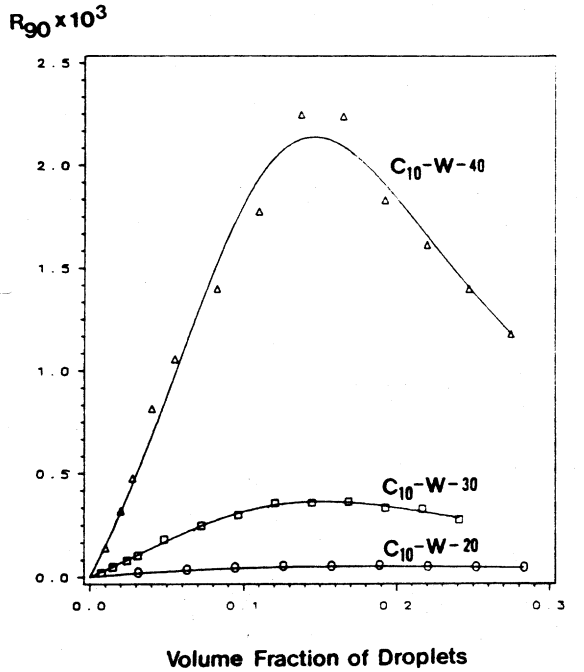

FIG. 5. The scattering intensity of microemulsion AOT–*n*-decane–water. The solid lines are theoretically calculated from Eq. [8].

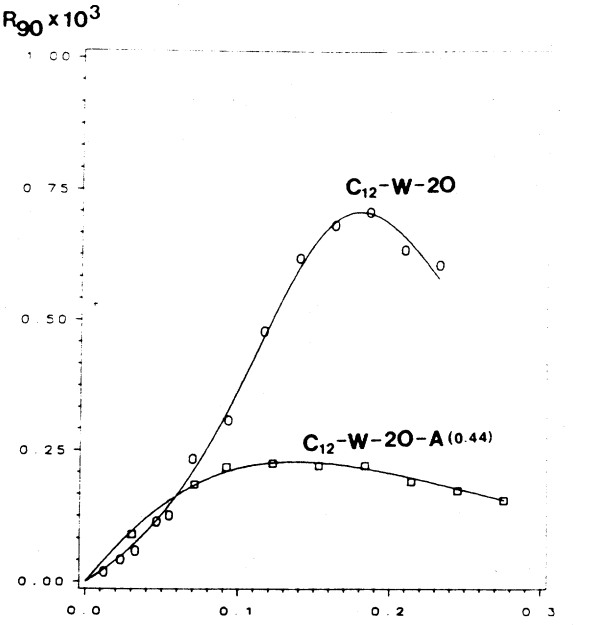

FIG. 6. The scattering intensity of microemulsion AOT–*n*-dodecane–water. The solid lines are theoretically calculated from Eq. [8].

TABLE III

Summary of the Results Obtained by Intensity Measurements

Samples	a	R^a (Å)	R_{hs} (Å)	A	B	$A^H \times 10^{12}$ (erg)	α^{th}	α^b
C_{10}-W-20	0.736	60.0	54.2	−3.5	3.3	1.11	0.2	−4.7
C_{10}-W-30	0.868	70.0	66.8	−10.8	−2.4	4.59	−2.9	−5.6
C_{10}-W-40	0.894	90.0	86.7	−13.8	−5.2	4.21	−4.4	−7.9
C_{12}-W-20	0.726	62.9	56.5	−17.7	−7.1	4.63	−5.0	−13.9
C_{12}-W-20-A(0.44)	0.950	66.7	65.6	−5.0	2.9	3.18	−0.5	−5.4

[a] R_H determined from QELS was taken as the radius of droplets.
[b] Obtained from the diffusion coefficients measurements.

Huang *et al.* (54) in an AOT–*n*-octane–water system. By applying a square well potential to interpret their small angle neutron scattering data, these authors found that the width of a potential well is a very short distance of about 3 Å. The small difference of 1.1 Å observed in C_{12}-W-20-A(0.44) is somewhat surprising, but consistent with the picture that the interfacial film became more rigid by the incorporation of Arlacel-20 molecules.

One can also calculate the Hamaker constant, A^H, from the value of A determined in the above study by using the equation (22, 25–26)

$$\frac{A^H}{kT} = -3Aa\left(\frac{R}{R_w}\right)^3\left\{\frac{1}{4}\ln\frac{s-1}{s+1} - s - s^3\ln\frac{s^2-1}{s^2}\right\}^{-1}, \quad [29]$$

where $R_w = R - l_c$, $l_c = 10.4$ Å, and $s = R_{hs}/R_w$. As shown in Table III, the calculated values of A^H are in good agreement with those obtained in AOT–*n*-heptane–brine (26) and other quaternary systems containing single chain surfactant (19–25). Thus, these results further confirmed that the long-range van der Waals attraction cannot account for the large Hamaker constants observed, as have been reported by many researchers (19–26).

III.2.3. Validity of Dilution

One of the fundamental assumptions in the above study is that all of the surfactant molecules are at the interface. Such an assumption is certainly not always true since the chemical equilibrium conditions of surfactant molecules dictate that the surfactants at interface must coexist with a dilute surfactant solution in both bulk phases (55). The possible effects of this discrepancy are discussed as follows. For the calculation of volume fraction, such an assumption is reasonable, since the surfactant concentration in continuum is too small (CMC of AOT in *n*-decane is about 0.225 m*M* (53)) compared with the amount of surfactant we used. Bedwell and Gulari (26) have suggested that the characteristic droplet size may decrease at high dilutions of samples due to the loss of water and/or surfactant to the continuous medium. Cazabat and Langevin (19) have shown that the theoretical value of the virial coefficient of diffusion, α^{th}, can be approximately related to A by

$$\alpha^{th} = (2 + A/2)a. \quad [30]$$

From the values of A and a determined by the intensity measurements, we can calculate α^{th} and compare it with those determined by the diffusion coefficients measurements. As shown in Tables II and III, we found that α is always smaller than α^{th} in five samples studied. Note that the diffusion coefficient measurement was done at a very dilute concentration range to apply the Stokes–Einstein relationship and D_0 was obtained by extrapolation to infinite dilution. On the other hand, the intensity measurements covered a wide concentration range

and the lowest volume fraction was greater than 0.035. Thus, we suspect that the discrepancy could be due to the loss of surfactant and/or water during high dilution so that diffusion coefficients were overestimated in very low concentration regions. As a result, the values of α determined were smaller than α^{th}.

III.3 Results Obtained from q-Dependent Analysis

We also measured the apparent diffusion coefficients, D, at varying angles from 30° to 150°. These q-dependent data were fitted with Eqs. [23] to [28] to determine the values of R_H, R_{hs}, and ϵ. This procedure was applied to most of the samples studied by the dilution method. In addition, two new samples were studied in the presence of alcohols. The results are summarized in Table IV. As shown in Fig. 7, the fitting of data is reasonably good for all the systems studied. However, one must be cautious of the following point before making any conclusion. That is, the dependence of D on the scattering angle is usually very weak for systems with low volume fraction and small droplet size, so that the observed variation of D may be within the experimental error, as shown in Fig. 8, where line 7 of Fig. 7 was magnified to show the quality of data against fitting. Therefore, the accuracy of the results from such fitting is open to question.

This error is particularly magnified when one compares the fitted values of B with those determined by intensity measurements. Although the trend of variation in B was still consistent with the results of intensity data, the quantitative values were in poor agreement. Thus, the large experimental error compared with the weak q-dependence essentially makes the fitted potential parameter values meaningless. However, the hydrodynamic radii obtained by such fitting are relatively close to those determined by dilution method, indicating that the concentration dependence has been approximately corrected through such a procedure. In fact, one can compare these results with those corrected by some available theoretical relationship such as that derived by Altenberger (56),

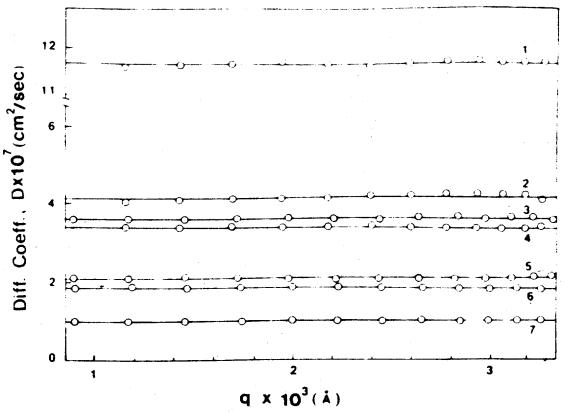

FIG. 7. The diffusion coefficients of microemulsions as functions of scattering angle. The samples measured were coded numerically as follows: 1, C_7-W-20; 2, C_7-W-40; 3, C_{10}-W-20-H (0.47); 4, C_7-W-60; 5, C_{10}-W-20; 6, C_{12}-W-20-A (0.44); 7, C_{12}-W-20.

TABLE IV

Summary of the Results Obtained by q-Dependent Analysis

Samples	ϵ/kT	R_{hs} (Å)	R_H (Å)	B	α
C_7-W-20	−0.20	44.5	48.9	8.5	1.9
C_7-W-40	1.39	71.7	79.5	−0.8	−3.6
C_7-W-60	1.15	79.0	90.0	−0.3	−5.2
C_{10}-W-20	1.19	45.6	56.8	−9.0	−8.7
C_{10}-W-20-P(0.38)	1.26	52.5	64.7	−9.6	−9.1
C_{10}-W-20-H(0.47)	1.05	29.5	37.5	−7.6	−7.9
C_{12}-W-20	2.06	64.0	75.7	−28.0	−20.0
C_{12}-W-20-A(0.44)	0.73	57.0	66.0	−1.0	−3.6

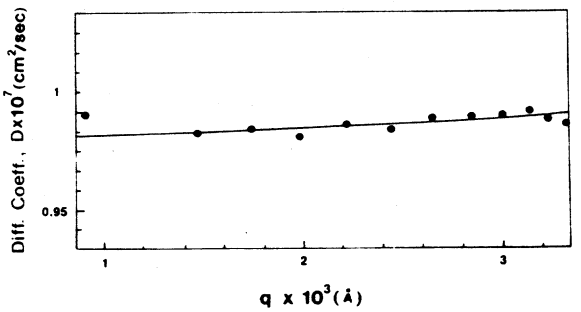

FIG. 8. The magnification of line 7 in Fig. 7. Note that the theoretical calculation (solid line) predicted a very small variation in D on changing scattering angle, which was within the experimental error.

$$\frac{D}{D_0} = \frac{[1 - 6\phi(1 - 2.2\phi)]}{(1 - 8\phi + 3.4\phi^2)}. \quad [31]$$

Table V shows the comparison of R_H determined by the dilution method, q-dependent analysis, and corrected by Eq. [31]. If one assumes that the radii determined by the dilution method are correct then it is clear that the correction by q-dependent fitting is better than by Altenberger's equation, at least for the systems studied here. Such surprising results are consistent with the observation of Chang and Kaler (35), who reported that the droplet size determined from such fitting seemed to be relatively insensitive to the potential form assumed.

This procedure was also applied to two other samples with a small amount of alcohols, where titration is difficult and inaccurate so that the dilution method is not applicable. The results showed that the addition of short chain alcohol, n-propanol, decreased the value of α, while long chain alcohol, n-heptanol, increased the value of α (compared to the value obtained by the same method for AOT–decane–water). It is to be noted that the addition of short chain alcohol increased the droplet size, while the long chain alcohol n-heptanol significantly decreased the droplet size, although the amount of alcohols added was very small (see Table IV).

IV. CONCLUSIONS

We have used QELS and SLS to study the droplet size and the interdroplet interaction in microemulsion systems containing AOT by changing the molar ratio of water to surfactant, chain length of oil, salinity, or by adding cosurfactants. The following conclusions were supported by the experimental results.

1. The radius of microemulsion droplets is primarily determined by the amount of water added for a fixed surfactant concentration. The droplet radius increased linearly as n_w/n_s increased from 20 to 60. The proportional increase in radius confirmed that the total interfacial area is constant and is independent of the amount of water added if the surfactant concentration is fixed.

2. The increase in the chain length of oil increased the droplet size of microemulsions. The droplet size was also found to decrease slightly as salinity increased.

3. The addition of cosurfactant may increase or decrease the size of microemulsion droplets, depending on the chemical structure of the cosurfactant added. The addition of a nonionic surfactant, Arlacel-20, increased the droplet size.

4. The interaction became more attractive as one increased n_w/n_s or chain length of oil or decreased the salinity. The addition of short chain alcohol, n-propanol, increased the strength of attractive interaction, while the addition of long chain alcohol, n-heptanol, and long chain nonionic surfactant, Arlacel-20, decreased the strength of attraction.

TABLE V

Comparison of the R_H Determined by Different Methods

Samples	ϕ	Hydrodynamic radius, R_H (Å)			
		Uncorrected radius	Corrected by Eq. [31]	Corrected by q-analysis	Obtained by dilution
C_7-W-20	0.104	45.8	44.3	48.9	40.3
C_7-W-40	0.146	133.7	97.4	79.5	84.0
C_7-W-60	0.184	148.5	75.0	90.0	119.5
C_{10}-W-20	0.128	112.3	94.7	56.8	60.0
C_{12}-W-20	0.051	152.9	163.7	75.7	62.3
C_{12}-W-20-A(0.44)	0.144	80.6	59.5	66.0	66.7

5. The Hamaker constant determined from the intensity measurement again confirmed that long-range van der Waals attraction cannot account for the large Hamaker constant observed, which has been addressed by several previous researchers.

6. We also examined the feasibility of analyzing q-dependent data to determine the droplet size and the strength of interaction. Although the results obtained are generally in fair agreement with those obtained by the dilution procedure, one must be aware of the inaccuracy of the analysis that came from the instrumental limitation in measuring the angle dependence of apparent diffusion coefficient. Thus, one must be cautious and make an independent check, e.g., by the dilution method, before drawing any conclusion from such analysis.

ACKNOWLEDGMENTS

We are grateful to the National Science Foundation (Grant NSF-CPE 8005851), the American Chemical Society Petroleum Research Fund (Grant PRF-14718-ACS), and ALCOA Foundation for supporting this research. We also thank one of the reviewers for providing a reference (26) for comparison and discussion of results.

REFERENCES

1. Leung, R., Hou, M. J., Manohar, C., Shah, D. O., and Chun, P. W., *in* "Macro- and Microemulsions" (D. O. Shah, Ed.), Vol. 272, p. 325. ACS Symposium Series, Washington, DC, 1985.
2. Schulman, J. H., and Riley, D. P., *J. Colloid Sci.* **3,** 383 (1948).
3. Marsden, S. S., *in* "Surface Phenomena in Enhanced Oil Recovery" (D. O. Shah, Ed.), p. 151. Plenum, New York, 1981.
4. Schulman, J. H., and Friend, J. A., *J. Colloid Interface Sci.* **4,** 497 (1949).
5. Graciaa, A., Lachaise, J., Chabrat, P., Letamendia, L., Rouch, J., and Vaucamps, C., *J. Phys. Lett.* **39,** L235 (1978).
6. Bowcott, J. E., and Schulman, J. H., *Z. Elektrochem.* **59,** 283 (1955).
7. Miller, C. A., Hwan, R.-N., Benton, W. J., and Fort, T., Jr., *J. Colloid Interface Sci.* **61,** 547 (1977).
8. Bansal, V. K., Chinnaswamy, C., Ramachandran, C., and Shah, D. O., *J. Colloid Interface Sci.* **72,** 524 (1979).
9. Gillberg, G., Lehtinen, H., and Friberg, S., *J. Colloid Interface Sci.* **33,** 40 (1970).
10. Chou, S. I., and Shah, D. O., *J. Phys. Chem.* **85,** 1480 (1981).
11. Raey, J. C., and Buzier, M., *in* "Surfactants in Solution" (K. L. Mittal and B. Lindman, Eds.), Vol. 3, p. 1759. Plenum, New York, 1984.
12. Kaler, E. W., Bennet, K. E., Davis, H. T., and Scriven, L. E., *J. Chem. Phys.* **79,** 5873 (1983).
13. Kaler, E. W., Davis, H. T., and Scriven, L. E., *J. Chem. Phys.* **79,** 5685 (1983).
14. Cebula, D. J., Ottewill, R. H., Ralston, J., and Pusey, P. N., *J. Chem. Soc. Faraday Trans.* **77,** 2585 (1981).
15. Dvolaitzky, M., Guyot, M., Lagues, M., Le Pesant, J. P., Ober, R., Sauterey, C., and Taupin, C., *J. Chem. Phys.* **69,** 3279 (1978).
16. Scriven, L. E., *Nature (London)* **263,** 123 (1976).
17. Guering, P., and Lindman, B., *Langmuir* **1,** 464 (1985).
18. Tabony, J., *Nature (London)* **319,** 400 (1986).
19. Cazabat, A. M., and Langevin, D., *J. Chem. Phys.* **74,** 3148 (1981).
20. Brunetti, S., Roux, D., Bellocq, A. M., and Bothorel, P., *J. Phys. Chem.* **87,** 1028 (1983).
21. Brouwer, W. M., Nieuwenhuis, E. A., and Kops-Werkhoven, M. M., *J. Colloid Interface Sci.* **92,** 57 (1983).
22. Cazabat, A. M., Langevin, D., and Pouchelon, A., *J. Colloid Interface Sci.* **73,** 1 (1980).
23. Cazabat, A. M., Langevin, D., Meunier, J., Abillon, O., and Chatenay, D., *in* "Macro- and Microemulsions" (D. O. Shah, Ed.), Vol. 272, p. 75. ACS Symposium Series, Washington, DC, 1985.
24. Agterof, W. G. M., van Zomeren, J. A. J., and Vrij, A., *Chem. Phys. Lett.* **43,** 363 (1976).
25. Calje, A. A., Agterof, W. G. M., and Vrij, A., *in* "Micellization, Solubilization and Microemulsions" (K. L. Mittal, Ed.), Vol. 2, p. 779. Plenum, New York, 1977.
26. Bedwell, B., and Gulari, E., *J. Colloid Interface Sci.* **102,** 88 (1984).
27. Zulauf, M., and Eicke, H.-F., *J. Phys. Chem.* **83,** 480 (1979).
28. Eicke, H.-F., Kubik, R., Hasse, R., and Zschokke, I., *in* "Surfactants in Solution" (K. L. Mittal and B. Lindman, Eds.), Vol. 3, p. 1533. Plenum, New York, 1984.
29. Fletcher, P. D. I., Robinson, B. H., Bermejo-Barrera, F., Oakenfull, D. G., Dove, J. C., and Steytler, D. C., *in* "Microemulsions" (I. D. Robb, Ed.), p. 221. Plenum, New York, 1982.
30. Gulari, E., Bedwell, B., and Alkhafaji, S., *J. Colloid Interface Sci.* **77,** 202 (1980).
31. Bedwell, B., and Gulari, E., *in* "Solution Behavior of Surfactants" (K. L. Mittal and E. J. Fendler, Eds.), p. 883. Plenum, New York, 1982.

32. Nicholson, J. D., and Clarke, J. H. R., *in* "Surfactants in Solution" (K. L. Mittal and B. Lindman, Eds.), Vol. 3, p. 1663. Plenum, New York, 1984.
33. Graciaa, A., Thesis, Universite de Pau, 1978.
34. Graciaa, A., Lachaise, J., Martinez, A., Bourrel, M., Chambu, C., *C.R. Hebd. Seances Acad. Sci. Ser. B* **282,** 547 (1976).
35. Chang, N. J., and Kaler, E. W., *Langmuir* **2,** 184 (1986).
36. Brown, J. C., Pusey, P. N., and Dietz, R., *J. Chem. Phys.* **62,** 1136 (1975).
37. Koppel, D., *J. Chem. Phys.* **57,** 4814 (1972).
38. Percus, J. K., and Yevick, G. J., *Phys. Rev.* **110,** 1 (1958).
39. Carnahan, N. F., and Starling, K. E., *J. Chem. Phys.* **51,** 635 (1969).
40. Barker, J. A., and Henderson, D., *J. Chem. Phys.* **47,** 2856 (1967).
41. Hou, M. J., and Shah, D. O., *Langmuir* **3,** 1086 (1987).
42. Corti, M., and Degiorgio, V., *J. Phys. Chem.* **85,** 711 (1981).
43. Felderof, B. U., *J. Phys. A* **11,** 929 (1978).
44. Cazabat, A. M., *J. Phys. Lett.* **44,** L593 (1983).
45. Fijnaut, H. M., *J. Chem. Phys.* **74,** 6857 (1981).
46. Lemaire, B., Bothorel, P., and Roux, D., *J. Phys. Chem.* **87,** 1023 (1983).
47. Roux, D., Bellocq, A. M., and Bothorel, P., *in* "Surfactants in Solution" (K. L. Mittal and B. Lindman, Eds.), Vol. 3, p. 1843. Plenum, New York, 1984.
48. De Gennes, P. G., and Taupin, C., *J. Phys. Chem.* **86,** 2294 (1982).
49. Hamaker, H. C., *Physica* (Amsterdam) **IV,** 1058 (1937).
50. Israelachvili, J. N., Mitchell, D. J., and Ninham, B. W., *J. Chem. Soc. Faraday Trans. 2* **72,** 1525 (1976).
51. Mukherjee, S., Miller, C. A., and Fort, T., Jr., *J. Colloid Interface Sci.* **91,** 223 (1983).
52. Huh, C., SPE/DOE, Reprint 10728, 1982.
53. Kotlarchyk, M., Huang, J. S., and Chen, S., *J. Phys. Chem.* **89,** 4382 (1985).
54. Huang, J. S., Safran, M., Kim, M. W., and Grest, G. S., *Phys. Rev. Lett.* **53,** 592 (1984).
55. Blankschtein, D., Thurston, G. M., and Benedek, G. B., *Phys. Rev. Lett.* **54,** 955 (1985).
56. Altenberger, A. R., *Chem. Phys.* **15,** 269 (1976).